Astron. Astrophys. 204, 242–252 (1988)

ASTRONOMY AND ASTROPHYSICS

Proto-planetary nebulae: the case of CRL 618

V. Bujarrabal, J. Gómez-González, R. Bachiller, and J. Martín-Pintado *

Centro Astronómico de Yebes (OAN-IGN), Apartado 148, E-19080 Guadalajara, Spain

Received December 16, 1987; accepted March 19, 1988

Summary. We have observed mm-wave emission from different molecules in the proto-planetary nebulae (PPNe) CRL 618 and CRL 2688. CRL 618 presents a very rich spectrum: in this source we have detected ^{12}CO, ^{13}CO, CS, SiO, C_2H, HCN, HNC, HCO^+, C_3N, C_3H_2, C_4H (tentative), HC_3N ($v=0$, $v7=1$, 2, $v6=1$), CH_3CN, and HC_5N; all of them are new detections, except CO and HCN. The excitation characteristics of the lines (in particular the vibrationally excited ones) show that the gas and dust in CRL 618 are significantly hotter than in CRL 2688, OH 231.8+4.2 and IRC+10216. Molecular abundances in CRL 618, as determined from our observations, are quite different from those in IRC+10216 and CRL 2688. These differences can be explained assuming that photodissociation by the stellar UV is acting in CRL 618 (particularly interesting are the high abundance of HCO^+ and the low HCN/HNC abundance ratio). The high temperature and photodissociation in this object should be related to the state of evolution, CRL 618 being probably more evolved than CRL 2688 and IRC+10216, but less than many other PPNe which practically lack molecular emission (see Paper I). The age of CRL 618 as PPNe is probably $\sim$200 yr, to be compared to the transit time (from AGB star to planetary nebula) which we deduce to be $\sim$1000 yr. Implications on late stages of stellar evolution are discussed, under a general picture of PPNe structure and evolution.

Key words: interstellar medium: molecules – stars: late-type – stars: circumstellar matter – planetary nebulae

1. Introduction

Proto-planetary nebulae (PPNe) have attracted a lot of attention in the last years, both from the theoretical and observational points of view. PPNe are supposed to represent the evolutionary transition from AGB stars to planetary nebulae (PNe), once the high mass loss characteristic of the last stages of the red giant evolution (superwind regime) has removed most of the stellar atmosphere, leaving exposed the hot and reduced nucleus (see, for instance, the general picture presented by Kwok, 1986). PPNe are one of the most interesting class of objects in the sky from the observational point of view. An important case is that of molecular radio observations of PPNe. With the arrival of large millimeter-wave telescopes, particularly the 30-m IRAM telescope, the millimeter spectra of some of these objects (CRL 618, CRL 2688, OH 231.8+4.2; see Lucas et al., 1986; Morris et al., 1987 and data in this paper) have been revealed as a true line forest, with features of (often unexpected) molecules as well as recombination lines. Surprisingly enough, for other PPNe (M1-91, M1-92, M2-9, NGC 2346, Red Rectangle; see Bachiller et al., 1988, Paper I) the molecular lines are practically nonexistent.

The goal of this paper is to analyse the molecular emission from PPNe, paying special attention to the case of the most interesting of these objects, CRL 618. We shall also try to draw conclusions on the physical conditions and state of evolution of these objects from the molecular observations.

We shall now summarize the observational features of PPNe, in order to adopt a practical characterization that will be useful for the following analysis.

1.1. *Presence of a bipolar structure in the visible*

In general this is composed of two bright lobes of partially ionized material. The continuum emission is often the reflected light from the star. Many spectral features are also detected. The existence of the lobes by itself implies that the star is surrounded by circumstellar (diffuse) matter. The analysis of the excitation requirements for the nebulae allows to place the central stars in the PPNe band of the HR diagram (the stars being in particular significantly hotter than red giants). See for more details Herbig (1975), Ney et al. (1975), Westbrook et al. (1975), Calvet and Cohen (1978), and Cohen (1983). Polarization in the optical and IR is detected in both continuum and lines; it also indicates reflected light in a bipolar structure (Schmidt and Cohen, 1981; Cohen and Schmidt, 1982; Heckert and Zeilik, 1983; Aspin and McLean, 1984).

1.2. *Strong far-infrared emission*

Fluxes as high as 1000 Jy are often detected. The maximum of the IR emission is in general found at 50–100 μm, corresponding to a dust temperature of 150–250 K. This also indicates the presence of diffuse dusty matter. See for instance Ney et al. (1975), Westbrook et al. (1975), Pottasch (1984), Soptka et al. (1985), and Kwok et al. (1986). The large IR intensity means that the UV opacity of the cicumstellar dust is high and it absorbs most of the stellar luminosity, suggesting a shell denser (less evolved) than those in standard PNe.

Send offprint requests to: V. Bujarrabal

* Also at IRAM, Av. Divina Pastora 7, E-18012 Granada, Spain

1.3. *Molecular line emission*

In the objects presenting this characteristic, many lines are detected corresponding to molecules such as CO, HCN, HC_3N, HC_5N, HC_7N, NH_3, OH, HCO^+, etc. The lines are mostly detected at millimeter wavelengths. The high number of molecular lines indicates that the circumstellar matter is relatively cool and has not been exposed to the stellar UV radiation (see Sect. 3; this requirement explains why molecules are so difficult to detect in PNe). The molecular line profiles and extension are similar to those observed in very evolved red giants, suggesting the same kind of circumstellar shell. See Baud (1981), Diamond et al. (1983), Beckwith et al. (1984), Lucas et al. (1986), Kawabe et al. (1987), Morris et al. (1987), next section in this paper and Paper I.

1.4. *No connection to interstellar H II region complexes and clouds*

This is opposed to what happens for young objects as bipolar molecular outflows, HH objects, or young reflection nebulae. See Calvet and Cohen (1978), Allen et al. (1980), this paper. This property means that the above mentioned diffuse matter in PPNe is a circumstellar shell ejected by an evolved object.

1.5. *Variability in the visible and radio continuum*

An increase of visual magnitude and radio intensity is observed in some objects. Such an increase implies that the object is rapidly evolving towards a high temperature, in the sense expected for PPNe. However, the periodic variability, typical of late type stars, is in general not observed. The presence of radio continuum indicates the existence of a compact H II region, and hence, a relatively early spectral type. See Gottlieb and Liller (1976), Kwok and Bignell (1984), Pottasch (1984). Habing and van der Veen (1986), and Martin-Pintado et al. (1988, Paper II)

It is worth noting that, to our knowledge, only in one of these objects, CRL 618, all of these characteristics have been detected: the identification of an object as a PPN is usually done only from the detection of two or three of the above characteristics.

We present our molecular observations in Sect. 2. The astrophysical results are discussed in Sect. 3, and some general conclusions can be found in Sect. 4. The transit time (from red giant to planetary nebula) and the local abundance of PPNe are discussed in the Appendix.

2. Molecular observations of PPNe

The observations presented here were made using the 30-m IRAM radiotelescope in Granada (Spain). The characteristics of the telescope and the observational procedure are described in Paper I.

We have detected in CRL 618 the molecules ^{12}CO, ^{13}CO, CS, SiO, C_2H, HCN, HNC, HCO^+, C_3N, C_3H_2, C_4H (tentative), HC_3N: $v=0$ (*J*: 8-7, 10-9, 12-11, 17-16, 25-24), $v_7=1$, 2, $v6=1$, CH_3CN and HC_5N: *J*: 35-34, 41-40; all of them are new detections except for CO and HCN (Lo and Bechis, 1976; Deguchi et al., 1986). We consider particularly interesting the detection of the ion HCO^+, for the first time in a carbon-rich object, as well as the high number of vibrationally excited lines of HC_3N (all of them were unknown in the circumstellar medium, $v_7=2$ lines were only detected in Orion A, see Goldsmith et al., 1985). Upper limits were obtained for other molecules, such as $C^{18}O$ and OCS (our upper limit for $C^{18}O$ is compatible with the tentative detection by Wannier and Sahai, 1987). The observed transitions and the line parameters are shown in Table 1 a. The lsr velocity centroid for the detected lines is $\sim -21\,km\,s^{-1}$. The profile area and the peak intensity were obtained from gaussian fitting, the rms noise was calculated in most of the cases after degrading the resolution to 2 MHz. Figure 1 is an example of our spectra. In this figure we show the same spectrum also for CRL 2688 and IRC + 10216, two objects that are, as explained below, probably less evolved than CRL 618. The differences in the line ratios are striking and the figure shows graphically some of the chemical and excitation differences discussed in the following sections.

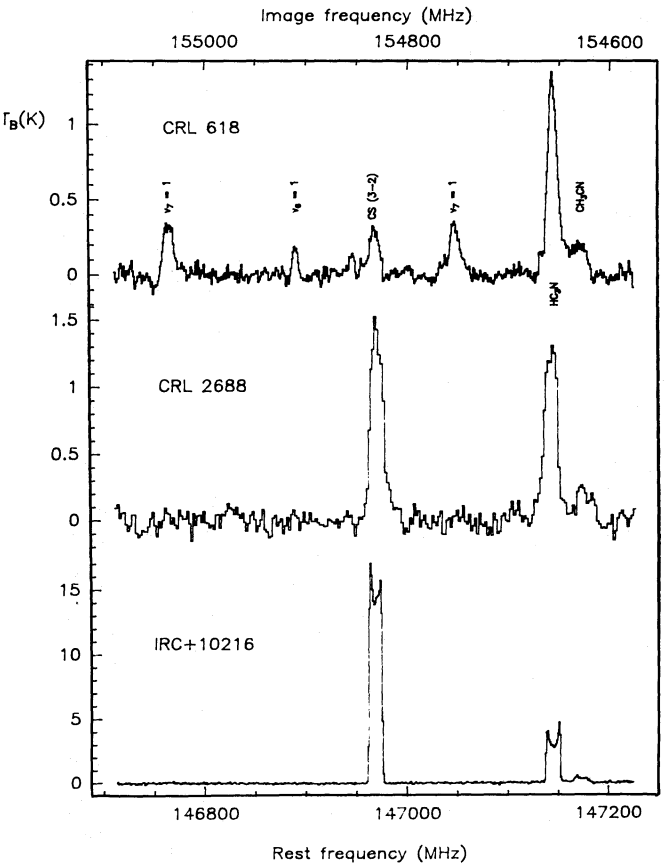

Fig. 1. Spectra at 147 GHz of CRL 618, CRL 2688, and IRC + 10216. Lines of HC_3N, in the ground and vibrationally excited levels ($v_7=1$, $v_6=1$), CS and CH_3CN are detected. (The image frequencies are calculated for CRL 618)

We have mapped the envelope of CRL 618 in certain strong lines: CO (2−1, 1−0), ^{13}CO (2−1, 1−0), HCN (1−0) and HC_3N (17−16). In every case the emission distribution seems comparable or larger than our beam and is essentially spherical, though in the inner region a slight elongation in the direction of the lobes is sometimes observed (see also Paper I). In Figs. 2 and 3 we show representative maps. Taking into account the broadening of the molecular extension produced by the beam size, we find molecular extensions ranging from 10″ in HC_3N (map width: ~19″; beam width: ~15″; pointing errors: ≦2″ in absolute value, probably smaller for relative positions) to 20″ in CO (see also Paper I). It is remarkable that the molecular emission and the optical lobe extensions are very similar. We note in the CO (2−1) spectrum map (Fig. 2) that the profiles are slightly shifted from one side to the other of the bipolar structure, suggesting that the molecular gas follows more or less the outflow detected in the visible (Westbrook et al., 1975), see also Paper I.

Table 1a. Molecular observations of CRL 618

Molecule	Transition	T_{mb} (K)	Sigma (K)	Area (K km s^{-1})
CO	1–0	4.4	0.05	114.0
	2–1	9.3	0.15	250.0
^{13}CO	1–0	0.5	0.02	14.2
	2–1	1.8	0.2	51.0
C^{18}O	1–0	<0.06	0.02	
CS	2–1	<0.15	0.05	
	3–2	0.3	0.02	6.6
SiO	(v = 0) 2–1	0.09	0.01	1.8
SiO	(v = 1) 2–1	<0.3	0.1	
CCH	3/2–1/2	0.13	0.01	2.2
HCN	1–0	0.9	0.02	20.1
HNC	1–0	0.92	0.04	19.1
HCO$^+$	1–0	0.7	0.03	14.5
C_3N	19/2–17/2	0.13	0.02	2.7
C_3N	21/2–19/2	0.1	0.02	2.1
C_3H_2	2(1, 2)–1(0, 1)	0.1	0.02	3.2
C_3H_2	4(3, 2)–4(2, 3)	0.09	0.02	1.8
C_4H	19/2, 9–15/2, 8	~0.06	0.02	
HC_3N	8–7	0.7	0.04	13.8
	10–9	0.8	0.02	15.6
	12–11	0.85	0.03	17.3
	17–16	1.1	0.02	27.5
	25–24	1.2	0.07	29.9
	(v_7 = 1) 10–9 lflf	0.2	0.02	3.4
	(v_7 = 1) 10–9 lele	0.2	0.02	3.2
	(v_7 = 1) 12–11 lflf	0.2	0.03	2.6
	(v_7 = 1) 17–16 lflf	0.2	0.02	7.4
	(v_7 = 1) 17–16 lele + (v_6 = 1) 17–16 lflf	0.3	0.02	7.6
	(v_7 = 1) 24–23 lflf	0.4	0.07	7.9
	(v_7 = 1) 12–11 lele + (v_6 = 1) 12–11 lflf	0.17	0.03	3.3
	(v_6 = 1) 12–11 lele	0.2	0.03	1.2
	(v_6 = 1) 17–16 lele	0.2	0.02	2.3
	(v_7 = 2) 12–11	0.06	0.015	1.1
CH_3CN	8(0)–7(0) + 8(1)–7(1)	0.2	0.02	
HC_5N	35–34	0.27	0.02	5.1
	41–40	0.26	0.03	6.7
	84–83	<0.2	0.07	

Line parameters obtained from the observations of CRL 2688 are shown in Table 1b, they were determined using the same methods as for CRL 618. CH_3CN is detected for the first time in the circumstellar medium. The lsr velocity centroid of the lines in CRL 2688 is ~ -35 km s^{-1}. In Fig. 1 we also represent, as mentioned earlier, some lines observed in CRL 2688. For observations of other PPNe mentioned in the text, see Paper I.

3. The envelopes of PPNe: CRL 618

The molecular envelope of CRL 618 is probably the most interesting one. We shall now discuss the consequences for the CRL 618 envelope derived from the observations presented here and from other published data. A comparison with other envelopes is also presented.

3.1. *Rotational temperature*

We have presented in Table 1a a certain number of molecules for which several transitions were observed. In principle, from the line intensity ratios, one can derive a "rotational temperature" representing the excitation temperature of the rotational transitions. As we shall discuss below, this rotational temperature is an interesting parameter.

Table 1b. Molecular observations in the PPN CRL 2688

Molecule	Transition	T_{mb} (K)	Sigma (K)	area (K km s^{-1})
CO	1–0	10.1	0.2	266.
^{13}CO	1–0	0.8	0.1	27.
CS	3–2	1.5	0.04	43.4
HCN	1–0	6.5	0.1	175.
HC_3N	8–7	2.5	0.04	71.6
	12–11	2.4	0.04	75.2
	17–16	1.3	0.04	40.0
	($v_7=1$) 12–11 lflf	< 0.1	0.04	
	($v_7=1$) 12–11 lele	< 0.1	0.04	
	($v_7=1$) 17–16 lflf	< 0.1	0.04	
	($v_7=1$) 17–16 lele	< 0.1	0.04	
CH_3CN	8(0)–7(0) + 8(1)–7(1)	0.25	0.04	
HC_5N	41–40	< 0.1	0.04	

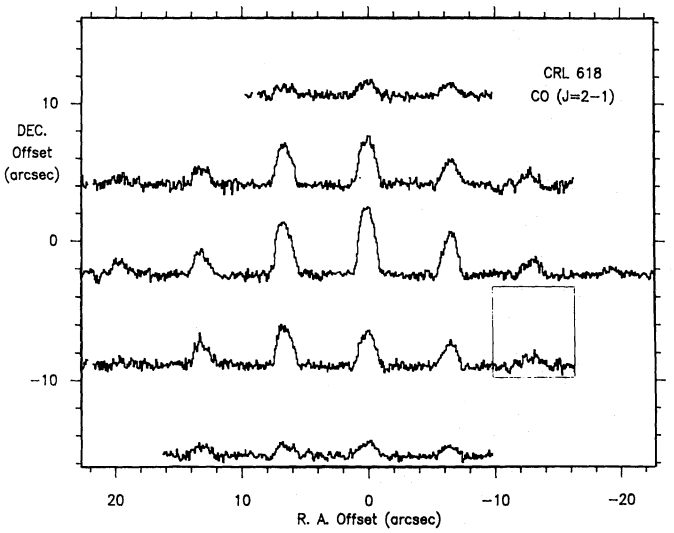

Fig. 2. Spectrum map of CRL 618 in the CO $J=2-1$ transition. The limits of the small box are: lsr radial velocity -80 to 40 km s^{-1} and main beam brightness temperature -1.5 to 11 K

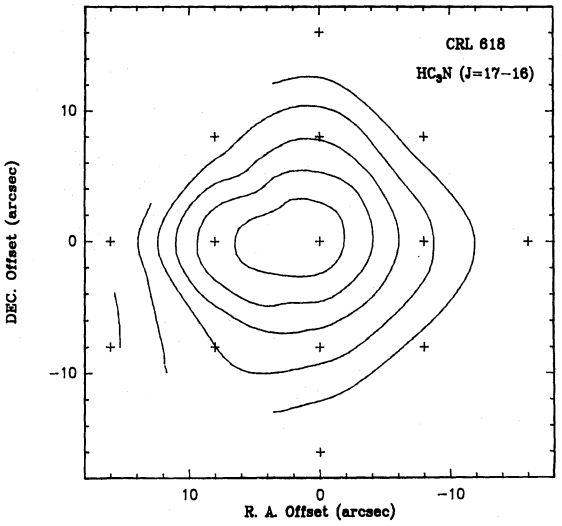

Fig. 3. Cartography of CRL 618 in the HC_3N J: 17–16 line. The first contour and interval are 2.5 and 5 K km/s

In this sense, the best information comes from HC_3N, whose $v=0$ transitions J=25–24, 17–16, 12–11, 10–9, and 8–7 were observed. From the maps discussed in Sect. 2, it appears that the extension of the HC_3N emission must be very similar to the antenna beam. The detected intensities are low, suggesting that the lines are optically thin. Hence the antenna temperature ratios (properly corrected) are probably a good measure of the respective upper level population and can be used to determine the rotational temperature. One could think that, due to the different beam sizes, the rotational temperatures so determined are somewhat overestimated if the source is not completely resolved. But what we find is that temperatures calculated using low J transitions are in fact smaller, which probably means that in lower frequency observations we are detecting lower temperature regions (emitting mostly in the lower J transitions). For ^{13}CO, the situation is similar. The ^{13}CO lines are not very intense, they are in particular significantly weaker than the ^{12}CO lines, which suggests that they probably are optically thin (see also Wannier and Sahai, 1987). We note that the ^{13}CO temperatures are subject to important errors due to the small difference in energy of the lines: 10% errors in the calibration may produce temperatures ranging from 50 K to 800 K. Using the antenna temperatures in Table 1a we have computed the rotational temperatures shown in Table 2. In Table 2 we also present the rotational temperature derived from the two HC_5N lines. In this case two calculations were made, one of them identical to that done for HC_3N, and the other considering the extension of the HC_5N (faint) emission to be much smaller than the beam. The second one is probably the most realistic, since HC_5N appears often as less extended than HC_3N.

The calculated rotational temperatures are quite similar, more so when one considers the very different excitation characteristics of the molecules and lines. In view of the values in Table 2, we shall

Table 2. Rotational temperatures in CRL 618

Molecule	Transition ratio	Rotational temperature (K)
HC_3N	J: 8 – 7/25 – 24	80
	J: 10 – 9/25 – 24	98
	J: 12 – 11/25 – 24	114
	J: 17 – 16/25 – 24	113
^{13}CO	J: 1 – 0/2 – 1	100 [a]
HC_5N	J: 35 – 34/41 – 40	670 81 [b]

[a] Uncertain value, see text
[b] Assuming the emission to be unresolved

adopt a rotational temperature of 90 K as a good approximation to the average (excitation) temperature in the region of molecular emission. This value is in good agreement with one of the components of the dust temperature deduced from IR measurements (see e.g. Paper II). One could think that the coincidence between the different rotational temperatures, and of these ones with the IR temperature, means that the molecular lines are practically thermalized and, then, that the rotational temperature is similar to the kinetic temperature. We must be cautious concerning this point. The volume densities expected for a mass loss rate of about $10^{-4} M_\odot$/yr (Knapp and Morris, 1985; see below), at a characteristic distance of 10^{17} cm from the center (equivalent to $\sim 4''$), are low, say $\sim 10^4$ cm^{-3} (assuming constant expansion velocity and mass loss, and spherical symmetry). It is difficult to believe that a molecule as hard to thermalize as HC_3N (e.g. Bujarrabal et al., 1981) can attain an excitation temperature of about 90 K for the observed high rotational lines only by means of collisional excitation. Probably, the strong IR emission from the dust in CRL 618 (Westbrook et al., 1975, Paper II) is contributing to a high degree to the detected rotational excitation (a similar phenomenon has been suggested to be acting for another IR source, IRC + 10216; see Morris, 1975; Deguchi and Uyemura, 1984; Nguyen-Q-Rieu et al., 1984a).

3.2. *Molecular abundances*

Once the rotational temperature is determined, and assuming that it is constant over all the rotational ladder and that the population of the vibrationally excited states is negligible, one can calculate the abundances of the observed molecules. ^{12}CO is particularly difficult to interpret due to its probably high opacity. We can however estimate the CO abundance assuming a $^{12}CO/^{13}CO$ ratio of ~ 50 (Knapp and Chang, 1985). We can even determine the mass loss rate assuming a $^{12}CO/H_2$ abundances ratio. If it is $\sim 6 - 8\ 10^{-4}$ (Lafont et al., 1981; Knapp and Morris, 1985) the mass loss so determined is compatible with the value obtained by Knapp and Morris (1985), $\dot{M} \sim 10^{-4} M_\odot$/yr. We note that the method we use depends only on the isotopic ratio $^{12}CO/^{13}CO$, but is relatively independent of envelope and excitation models, which are necessarily uncertain for these partially known objects. In Table 3 we present the calculated values of the relative abundances for the above mass loss rate, for CRL 618 as well as for other related objects and two representative clouds of the interstellar medium (see references in the table). For CRL 618 and CRL 2688 we have calculated the abundances assuming that the object is resolved, and also assuming that it is unresolved with a size (diameter, D) of 10″ (the spatial extension of CO, HCN, and HC_3N is known; for these molecules the first assumption is preferable). The discrepancies shown in the table give then an idea of the expected uncertainties due to the geometry. We note that for IRC + 10216 the quoted abundances were in general calculated for a resolved envelope, and that for OH 231.8 the abundances were calculated in the unresolved case.

As we can see in Table 3, many of the abundances in CRL 618 are significantly lower than those found in the IR star IRC + 10216, and even lower than for CRL 2688 (an object probably less evolved than CRL 618, see e.g. Calvet and Cohen), but slightly larger than those usually found in the interstellar medium (Guélin, 1987). On the other hand, the HCO^+ abundance in CRL 618 is much larger than that in IRC + 10216 and CRL 2688, and even larger than in the interstellar medium; it is the first time that HCO^+ is detected in a carbon-rich object. These facts suggest that, during the transit from AGB star to PN, the

Table 3. Molecular abundances in porto-planetary nebulae

Mol.	IS medium		CRL 618		CRL 2688		IRC + 10216	OH 231.8
	Ori A	TMC – 1	Res.	Size: 10″	Res.	Size: 10″		
^{13}CO	$2\ 10^{-6}$		$2\ 10^{-5}$	$6\ 10^{-5}$	$2\ 10^{-5}$	$9\ 10^{-5}$	$1\ 10^{-5}$	$1\ 10^{-4}$
CS	$1\ 10^{-9}$	$4\ 10^{-9}$	$2\ 10^{-8}$	$6\ 10^{-8}$	$6\ 10^{-8}$	$2\ 10^{-7}$	$2\ 10^{-7}$	$3\ 10^{-7}$
SiO	$1\ 10^{-8}$	$<4\ 10^{-10}$	$1\ 10^{-8}$	$4\ 10^{-8}$			$6\ 10^{-8}$	$8\ 10^{-8}$
C_2H	$5\ 10^{-9}$	$8\ 10^{-9}$	$5\ 10^{-7}$	$2\ 10^{-6}$	$9\ 10^{-7}$	$4\ 10^{-6}$	$2\ 10^{-6}$	
HCN	$8\ 10^{-8}$	$2\ 10^{-8}$	$1\ 10^{-7}$	$5\ 10^{-7}$	$4\ 10^{-7}$	$2\ 10^{-6}$	$1\ 10^{-5}$	$4\ 10^{-7}$
HNC	$1\ 10^{-9}$	$3\ 10^{-8}$	$1\ 10^{-7}$	$4\ 10^{-7}$			$8\ 10^{-8}$	$2\ 10^{-7}$
HCO^+	$5\ 10^{-9}$	$8\ 10^{-9}$	$4\ 10^{-8}$	$2\ 10^{-7}$	$<1\ 10^{-9}$	$<3\ 10^{-9}$	$<5\ 10^{-10}$	$8\ 10^{-8}$
OCS	$1\ 10^{-8}$	$2\ 10^{-9}$	$<1\ 10^{-7}$	$<5\ 10^{-7}$	$<4\ 10^{-8}$	$<2\ 10^{-7}$	und.	$1\ 10^{-6}$
C_3H	$<1\ 10^{-10}$	$1\ 10^{-9}$	$4\ 10^{-8}$	$2\ 10^{-8}$	$4\ 10^{-7}$	$2\ 10^{-7}$	$4\ 10^{-7}$	
C_3H_2			$4\ 10^{-7}$	$2\ 10^{-6}$				
C_4H	$<1\ 10^{-10}$	$3\ 10^{-8}$	$\sim 2\ 10^{-8}$	$\sim 8\ 10^{-8}$			$1\ 10^{-6}$	
HC_3N	$5\ 10^{-10}$	$6\ 10^{-9}$	$5\ 10^{-8}$	$2\ 10^{-7}$	$2\ 10^{-7}$	$8\ 10^{-7}$	$2\ 10^{-7}$	$<4\ 10^{-8}$
HC_5N	$3\ 10^{-11}$	$2\ 10^{-9}$	$3\ 10^{-8}$	$1\ 10^{-7}$	$<1\ 10^{-7}$	$<4\ 10^{-7}$	$8\ 10^{-8}$	
Refs.:	1		5		4 5		2 1	3

References: 1: Guélin (1987), 2: Lafont et al. (1981), 3: Morris et al. (1987), 4: observations from Lucas et al. (1986), 5: this paper

molecular envelope of CRL 618 is suffering a considerable chemical evolution, the chemical composition of the molecular gas being now closer to what is typical in interstellar clouds. This effect is probably due to the presence of a strong UV continuum from the central star, which leads to a chemistry dominated by photodissociation (e.g. Lafont et al., 1981). The striking high abundance of HCO^+, the very low HCN/HNC abundance ratio and the low HC_3N abundance (probably the best determined of the abundances) in CRL 618 is the best support to this thesis.

The abundances found in the oxygen-rich PPN OH 231.8 + 4.2 by Morris et al. (1987) are more or less similar to those found in our carbon-rich CRL 618, except for the larger abundance of some oxygenated molecules, as OCS.

3.3. *The vibrationally excited lines of HC_3N*

The intensities of the vibrationally excited lines in CRL 618 ($v_7 = 1$, 2; $v_6 = 1$) are particularly high, CRL 618 and Orion A being the only objects in the sky where $v_7 = 2$ lines have been detected. The determination of a vibrational temperature is however severely vitiated by the fact that the excited lines probably come from a reduced region, as compared to the $v = 0$ lines. We see, for example, that the the $v_6 = 1$ lines are systematically and significantly narrower than the $v = 0$ lines. Calculating, moreover, the vibrational temperatures from the integrated fluxes (the peak flux is often very affected by the noise), we notice very different vibrational temperatures for the different lines. The $v_6 = 1$ lines correspond to a vibrational temperature of 290 K, whereas both $v_7 = 1$ and $v_7 = 2$ lines are compatible with a temperature of 180 K (these figures are probably lower limits to the true vibrational temperature due to the different sizes of the emitting regions, mainly for the $v_6 = 1$ lines). The high excitation of the $v_6 = 1$ state is particularly interesting. This high excitation cannot be explained without invoking radiative vibrational excitation. The $v_6 = 1 \rightarrow v = 0$ radiative transition probability is large, with an Einstein coefficient A of $0.12\,s^{-1}$ ($A(v_7 = 1 \rightarrow 0) = 6\ 10^{-4}\,s^{-1}$, $A(v_7 = 2 \rightarrow 1) = 1.2\ 10^{-3}\,s^{-1}$, see Goldsmith et al., 1985). Consequently, an efficient collisional excitation would require densities of the order of $10^{10}\,cm^{-3}$, too large even at the inner boundary of the neutral envelope (0″.2–0″.4, see e.g. Paper II).

In addition, under a collisional excitation regime the vibrational temperature of the $v_7 = 1$, 2 lines is expected to be much higher than the $v_6 = 1$ one: Assuming the radiative deexcitation to be dominant and the population to be performed mainly from the ground state, the vibrational excitation is given by

$$x_u A \sim x_l n C \exp(-E/\mathrm{kT_k}),$$

where, x_u, x_l are the populations of the upper and ground states, C is the collisional deexcitation coefficient ($u \rightarrow 0$, $cm^3\,s^{-1}$), n is the total volume density, E is the energy of the u state, and T_K is the kinetic temperature. Then,

$$x_l/x_u \sim A/(C n \exp(-E/kT_K)$$

$$T_{ex} \sim E/\ln(A/(C n \exp(-E/kT_K)).$$

E, the energy of the excited state, is about 720 K for the $v_6 = 1$ state and 320 K for the $v_7 = 1$ one. For reasonable C coefficients (see Goldsmith et al., 1985) T_{ex} must always be smaller for $v_6 = 1$ than for $v_7 = 1$, 2; mainly due to the large $v_6 = 1 \rightarrow 0$ Einstein coefficient. Only when the collisions are strong enough to thermalize the vibrational lines, do the $v_6 = 1$ and $v_7 = 2$ states have the same excitation temperature. For example, using the Einstein and collisional coefficients discussed by Goldsmith et al. for a kinetic temperature $T = 300$ K, and a density $n = 10^7\,cm^{-3}$, we obtain $T_{ex}(v_7 = 1) \sim 110$ K, $T_{ex}(v_7 = 2) \sim 140$ K and $T_{ex}(v_6 = 1) \sim 75$ K.

However, in the case of radiative excitation, the vibrational state population is given by

$$x_l/x_u \sim (\exp(E/kT_d) - 1 + W)/W,$$

where for a given u state, l is the immediately lower level in the v scale, E is the energy between the u and l states, W is the dilution factor for the IR radiation as seen "by" the molecules (this factor, always $\leqq 1$, comes from the usual distance and opacity dilution effects), and T_d is the dust temperature. The Einstein coefficients cancel, since they enter both excitation and deexcitation. We can easily verify that the $v_6 = 1$ level has vibrational temperatures larger than the $v_7 > 0$ levels for all the physically meaningful combinations of parameters ($T_d > 0$ K, $W \leqq 1$). We accordingly conclude that at least the $v_6 = 1$ lines are populated by absorption of dust IR radiation with a radiation temperature of $\gtrsim 300$ K. For the less difficult to excite $v_7 > 0$ lines a minor contribution of the collisional excitation cannot be excluded.

On the other hand, the region emitting in the $v_6 = 1$ lines must be relatively large (though smaller than the $v = 0$ region). Assuming the rotational lines to be thermalized and optically thick, in order to produce a main-beam temperature of ~ 0.2 K for a beam of $\sim 20''$, the emitting region must have a radius of $\sim 0''.4$ (a size completely similar to the inner boundary of the neutral region), if the dust temperature and the excitation temperature are ~ 300 K (a value very similar to that deduced from the IR continuum by Westbrook et al., see also Paper II). Note that this size is a lower limit, since our hypotheses tend to produce an underestimate of the emitting size, and that the exciting dust region must be of about the same size as the $v_6 = 1$ region, since the W factor decreases rapidly due to geometrical reasons once the molecules get out of the IR emitting region. To explain the detected vibrational temperature of ~ 290 K for the $v_6 = 1$ lines, we must then assume the existence of hot dust of ~ 300 K occupying a region larger than about 0″.8, i.e. larger than about $2\ 10^{16}$ cm. If T_d is higher than 300 K, one deduces a smaller region, but the size variation is small: for $T_d = 600$ K, the minimal size is $\sim 1.5\ 10^{16}$ cm. In any case, the hot dust region seems to be very extended in CRL 618, for example, for IRC + 10216 such a region is only of the order of $6\ 10^{15}$ cm (e.g., Toombs et al., 1972).

3.4. *Envelopes around other PPNe*

As shown in Paper I (see also Knapp and Morris, 1985; Knapp, 1986), the molecular emission in many protoplanetaries is much weaker than that found in CRL 618: M1–91 has no detectable CO emission; M2–9, M1–92 and the Red Rectangle present very weak CO (and no other molecule); and NGC 2346 presents weak CO emission (~ 0.5 K) with a sizeable spatial extension. Nevertheless, a few objects, probably still less evolved than CRL 618, as OH 231.8 and CRL 2688, and of course IRC + 10216 and CIT-6, also present intense molecular lines. A summary of the molecular emission from PPNe is presented in Table 4, where "intense" means $T_a(\mathrm{CO}) \gtrsim 1$ K (30-m) or other molecules detected; references for molecular measurements are those quoted above in the text, or in the table.

One important characteristic of the PPN envelopes is that their linear size, measured from the optical image or from molecular emission maps (where it has been observed, see also Kawabe et al., 1987; Morris et al., 1987), is practically the same and quite constant from object to object, see Table 4. The average measured

Table 4. Closest possible proto-planetary nebulae

	Dist. (kpc)	Size (cm)	Mol. em.	Ident.	Ref.
IRC + 10216	0.3	$5\ 10^{+17}$	Intense	AGB?	Wannier et al.
IC 418	0.4	$1\ 10^{+17}$	Weak	PN??	Pottasch
Red Rectangle	0.4	$3\ 10^{+17}$	Weak		Cohen et al. (1975)
BD + 30° 3639	0.6	$5\ 10^{+16}$	–	PN??	Pottasch
Boomerang Neb.	0.8	$6\ 10^{+17}$	–		Taylor and Scarrot
OH 26.5 − 0.6	0.8	$1\ 10^{+17}$	Intense	AGB??	Baud
M 2 − 9	1.0	$5\ 10^{+17}$	Weak		Kwok et al. (1985)
NGC 7027	1.0	$7\ 10^{+17}$	Intense	PN??	Pottasch
NGC 6302	1.0	$1\ 10^{+18}$	Weak	PN??	Silvestro and Robberto
OH 231.8 + 4.2	1.3	$3\ 10^{+17}$	Intense		Morris et al.
CRL 2688	1.5	$7\ 10^{+17}$	Intense		Calvet and Cohen
Hen 401	1.5?	$6\ 10^{+17}$?	–		Allen
CRL 618	1.7	$5\ 10^{+17}$	Intense		Calvet and Cohen
NGC 2346	1.7	$1.5\ 10^{+18}$	Weak		Calvet and Cohen
FG Sge	1.8	$1\ 10^{+18}$	–	AGB?	Pottasch
Mz-3	1.8	$1.4\ 10^{+18}$	–		Cohen et al. (1978)
V 1016 Cyg	2.0	$1\ 10^{+16}$	Undet.	AGB?	Pottasch
Roberts 22	2.0	$2\ 10^{+17}$	–	young?	Allen et al.
M 3 − 28	2.3	$6\ 10^{+17}$	–	PN?	Calvet and Cohen
89 Her	2.6	–	Weak	AGB?	Likkel et al.
HD 161796	3.0	–	Weak	AGB?	Likkel et al.
SAO 163075	3.0	–	Weak	AGB?	Likkel et al.
M 1 − 92	3.0	$4\ 10^{+17}$	Weak		Herbig
M 1 − 91	3.1	$1\ 10^{+18}$	Undet.		Calvet and Cohen
IRC + 10420	3.4	$1\ 10^{+17}$	Intense	AGB?	Knapp and Morris
M 4 − 18	3.5	$<1\ 10^{+17}$	–	PN?	Goodrich and Dahari
OH 17.7 − 2.0	5.0	$2\ 10^{+17}$	Weak	AGB?	Diamond et al. (1985)
IRAS 09371 + 1212	5.0?	–	Weak	AGB?	Rouan et al. (1988)

size (D) is of about $7\ 10^{17}$ cm. This is also the case of the CO extension in IRC + 10216 ($\sim 5\ 10^{17}$ cm, e.g., Wannier et al., 1979), and in the young planetary nebulae NGC 7027 ($\sim 7\ 10^{17}$ cm, Knapp et al., 1982) and NGC 6302 ($\sim 10^{18}$ cm, Silvestro and Robberto, 1986; Zuckerman and Dyck, 1986), which are molecule-rich. This remarkable property holds in spite of the large uncertainties existing in the distance and in the definition of size, since images of different exposure times and characteristics must be used, see Jewitt et al. (1986). (Some young PNe do not present this property, possibly because the optically measured size for these objects represents a different physical parameter than for PPNe.) The larger discrepancies in bona fide PPNe relative to the canonical value $D \sim 7\ 10^{17}$ cm do not exceed a factor of two. We interpret this result as follows. A "normal" star of, say, $1\ M_\odot$ cannot maintain a superwind of $5\ 10^{-5}\ M_\odot$/yr during more than $\sim 10^4$ yr, before loosing its atmosphere. If the expansion velocity is 15 km s^{-1}, this dense envelope occupies at the moment of the superwind quenching a sphere of radius $4.5\ 10^{17}$ cm, i.e. the observed size of the nebulae.

The existence of a typical CO size allows us to calculate the expected dilution factor of the CO emission, which is, for example, of the order of 0.2 for M 1–92 and of the order of 1 for the Red Rectangle, M 1–91, NGC 2346 and M 2–9. If, moreover, one considers that the CO lines are at least partially saturated in CRL 618, the weak CO emission in certain PPNe can only be explained assuming either that CO is underabundant (in the sense that its extension and/or relative abundance is anomalously small), or that the kinetic temperature is very high, at least about 1000 K. It seems however very improbable that the molecular gas be heated up to such a high temperature at a distance from the star $> 10^{17}$ cm: molecules must then be underabundant for these low-emission objects. Further consequences of the CO observations in PNNe are presented in Paper I. In that work, we explain the low CO intensity in most PPNe on the basis of a time-dependent model of photodissociation due to the central star UV emission, predicting strong molecular depletion for PPNe older than a few hundred years (about 300). Measurements of radio continuum and recombination lines (compiled in Paper II, see also Kwok and Bignell, 1984) show the existence of an expanding inner shell of ionized material, whose lifetime is probably similar to the PPN age, at least under the PPN picture presented above. The kinetical time of such a shell indicates that the time spent by CRL 618 as a PPN must be of the order of 200 yr. If, as we discuss below, the time possibly spent by stars as PPNe is of the order of 1000 yr, we can understand in terms of this model of PPNe evolution why only a (nonnegligible) fraction of the protoplanetary nebulae present important molecular emission, and that CRL 618 is probably not an extraordinary object. We interpret it as just being evolved enough to present high excitation lines, but not enough to dissociate the molecules. [It is possible, however, that the "usual" PPNe phase occurs only in the evolution of relatively heavy objects, as discussed in the Appendix. CRL 618, in particular, may have a relatively heavy progenitor, as can be deduced from the high luminosity obtained by Calvet and Cohen (1978) or the discussion on the inner ionized region by Kwok and Bignell (1984).]

We have observed several molecular lines in CRL 2688 (Sect. 2, Table 1b). This object surrounds an A-type star and is probably less evolved than CRL 618 (e.g., Calvet and Cohen, 1978). Molecules like CO, CS, HC_3N, HC_7N, NH_3, etc. were already known in CRL 2688 (e.g., Lucas et al., 1986), CH_3CN is a new detection. Our CO, CS, and HC_3N ($J=8-7$, $12-11$) lines present the broad wings found in CO ($J=1-0$) by Kawabe et al. Using the three HC_3N lines presented here we can determine the rotational temperature as it has been done above for CRL 618. The possible combinations give $T_r \sim 25$ K, in good agreement with that determined by Nguyen-Q-Rieu et al. (1984b) using the (1, 1) and (2, 2) lines of ammonia. The temperature is similar in this object and in OH 231.8 + 4.2 (Morris et al., 1987), but the bulk of the molecular gas is significantly cooler than in CRL 618. It may be due to the probably smaller dust opacity in CRL 618, a consequence of its advanced evolution, which allows the heating of larger regions in its envelope (note that the total stellar luminosity varies only slightly along the PPNe path, e.g. Calvet and Cohen).

Assuming $T_r = 25$ K and $\dot{M} = 10^{-4}\, M_\odot$/yr (Knapp and Morris, 1985), we have determined the abundances of the different molecules in CRL 2688. The values are presented in Table 3, where we also include results from the analysis of 30-m data from Lucas et al. As quoted above, the abundances are in general quite close to those in IRC + 10216, supporting the idea that CRL 2688 is chemically less evolved than CRL 618.

4. Conclusions

From our study of CRL 618 and other PPNe, we conclude:

1. Certain PPNe present intense and rich molecular emission, including high-excitation lines, such as $v_7 = 1$, 2 and $v_6 = 1$ HC_3N lines, and relatively exotic molecules, as C_4H and CH_3CN. It is the case of the particularly interesting object CRL 618, and also of CRL 2688 (see also Lucas et al., 1986) and OH 231.8 (Morris et al., 1987).

2. The size of the optical and CO images of PPNe are quite similar and relatively constant from object to object; we found a typical size of about $7\ 10^{17}$ cm, with no discrepancy exceeding a factor of two.

3. CRL 618 is probably the most interesting molecular source. We have determined molecular abundances for ^{13}CO, CS, SiO, HCN, HNC, etc, see Table 3. These abundances are quite different from those known for the less evolved IRC + 10216, the differences being in general in the sense expected if photodissociation by UV photons from the central star is beginning to act in the CRL 618 envelope. Particularly interesting are the high abundance of HCO^+ and the low HCN/HNC abundance ratio. Photodissociation by stellar UV probably explains also why many PPNe (NGC 2346, M 2–9, Red Rectangle, etc) present very weak molecular emission: probably only objects younger than about 300 yr are molecule rich (see Paper I). The molecular abundances we found in CRL 2688 are however quite similar to those in IRC + 10216.

4. We find for CRL 618 a (rotational) temperature of ~ 90 K, averaged over the bulk of the molecular envelope, significantly larger than the values accepted for other objects such as CRL 2688 and OH 231.8 + 4.2 (~ 25 K).

5. Vibrationaly excited states observed in CRL 618 seem to be radiatively populated (this PPN is a very intense IR source). The region of high vibrational and IR temperatures (~ 300 K) must be quite extended (up to distances $> 2\ 10^{16}$ cm from the star), in order to explain the molecular emission.

6. We suggest, in summary, that an extended high-temperature region and a chemistry more and more dominated by photodissociation are effects of an advanced evolution of a proto-planetary object, both being produced by a decrease in the total dust opacity during the PPN phase, which allows a deeper penetration of the stellar emission.

7. The age of CRL 618 (as PPN) is about 200 yr (see Kwok and Bignell and Paper II), this object being probably less evolved than M 2–9, M 1–91, NGC 2346, Red Rectangle, etc, but more evolved than CRL 2688 and IRC + 10216. The transit time of PPNe, i.e. the time necessary for these objects for going from AGB stars to planetary nebulae, is probably ~ 1000 yr (see Appendix). The comparison of this value with the lifetimes given above, together with the evolutionary considerations, places the studied PPNe in a general picture of late stellar evolution. A picture that, without excluding other possible post-AGB evolutionary paths, like the evolution to RV Tau objects (Jura 1986), seems to yield a consistent view of the evolution of pre-planetary objects.

Appendix: the transit time

The amount of time necessary for stars to transit from the AGB last stages to planetary nebulae, i.e. the time spent by the stars in the proto-planetary stage, is an important but largely unknown parameter (e.g. Renzini, 1983; Schönberner, 1986). In Sect. 3.3, we have been compelled to use a typical value of the transit time (t_t) for comparison with the age of CRL 618 and for extracting conclusions about the different degrees of molecular richness of the objects. The nowadays abundant observational information on this problem allows however a relatively precise determination of the transit time (t_t). The transit times we shall obtain below must be considered as empirical values, mainly related to the evolution of the envelope.

A1. Methods for the determination of the transit time

The major problem in studying the possible values of t_t is that the definition of PPN is (perhaps necessarily) quite vague. We shall assume that, when the superwind regime "quenches", the large loss of cool mass ends and the denser part of the envelope begins to move away from the star (leaving a hole filled by a much hotter and less dense wind; we shall neglect in the following discussion the possibility of interacting winds, since the interaction effect is not well known and seems to be produced only in one direction, see Kwok and Bignell, 1984, Paper II). Around the star a PPN is already formed. As the envelope moves further away, its density decreases and the IR opacity drops. This favours molecule dissociation by the stellar UV, and the molecular emission sharply decreases. At the same time, the star, which is loosing the last part of its atmosphere, is becoming hotter. When the dust opacity in the visible and UV reaches unity, the dust only absorbs a fraction of the total stellar radiation. Consequently, the IR emission diminishes and at the same time the star and the inner ionized region become visible. The bipolar structure becomes often looser or undetectable. We have a typical PN. (In this approximative view, we can assume that a coupling between the dissipation of the envelope and the heating of the central star is probable, since they are practically equivalent phenomena.) We shall use this simplified picture to define and determine the transit time.

In determining the transit time we distinguish three different arguments:

A1.1. Kinematical life times for planetary nebulae

The interpretation of this parameter is difficult for several reasons. First, we do not know exactly what part of the envelope we are seeing as PN. Probably, the visible nebula includes at least the inner (dense) part of the red giant envelope, but we cannot be sure that it does not include outer regions (as we can expect for very evolved PNe), ejected much earlier. Second, we can only estimate what part of this time has been spent by the star as a true PN. Third, the expansion velocities used to calculate the PN kinematical times are in general larger by $\sim 70\%$ than the expansion velocities in AGB star envelopes. In any case, it seems clear that the kinematical time (t_K) of PNe is an approximate upper limit to t_t. To minimize the overestimation, we can choose among the observed t_K's those corresponding to objects which, according to its location in the $H-R$ diagram, are expected to be less evolved: the t_K for these objects are indeed usually the smallest. An inspection of the compilation of data by Pottasch (1984) reveals that for the different absolute magnitudes (i.e. the different evolutionary tracks) one can find objects with $t_K \sim 1000$ yr. Even if the interpretation of these kinematical times remains a problem, it seems justified to conclude that this value is a reasonable limit to the transit time, $t_t \lesssim 1000$ yr.

A1.2. Local spatial density of PPNe

Assuming that PPNe are the evolutionary link between red giants and PNe, and assuming a value for the local formation rate of PNe, the determination of the local spatial density (dl) of PPNe should indicate the time spent by the stars as protoplanetaries. However, the estimation of dl is still difficult: a) As we have already pointed out, the definition of PPN is not easy, and the confusion between PPNe and red giants or PPNe and PNe is often hard to resolve. b) The distance determination for these particular objects is in general very delicate. c) PNNe are still not sufficiently well studied to be sure that any list of objects represents a reliably complete set. We have, in any case, compiled in table 4 the nearest detected possible PPNe (to our knowledge), including distances (references in the table) and comments on the identification as PPN. (For IRAS 09371 + 1212 we obtain a distance $\gtrsim 5$ kpc, assuming that the optical and IR angular size, measured by Rouan et al. 1988, corresponds to the typical linear size of PPNe deduced above.) This list is not aimed to be complete, but we think it *is not severely* incomplete for small distances (~ 1.5 kpc). This is because, as we know, a fundamental characteristic of PPNe is that their IR emission is very strong for $\lambda \sim 25$–$60\,\mu$m. For instance, the IR fluxes in CRL 618 are larger than 1000 Jy at 25 μm and 60 μm. Many similar objects at $\lesssim 1.5$ kpc should be conspicuous in the IRAS catalogue. This is obviously not the case, an inspection of this catalog shows the presence of about 4 objects (besides galaxies, objects apparently associated with star-forming regions, known PPNe, etc) with maximum emission placed between 25 and 60 μm and larger than 100 Jy. We note moreover that in the recent extensive search for possible PPNe by Likkel et al. (1987), using IR and CO measurements, only candidates at distances of about 3 kpc were found.

In Table 5 we have included the number of "probable" and "possible" (in view of the difficult identification) PPNe for different distances, together with, as a comparison, the expected number of objects for $dl = 2\ 10^{-9}\ \mathrm{pc}^{-3}$ and assuming a galactic height of 0.25 kpc, as for PNe. We note that the height scale is not well known, but as long as we take the same for PNe and PNNe, the resulting transit time will not depend on this ill-defined parameter. Recalling that our list is probably not complete and that the birthrate of PNe is $\sim 2\ 10^{-12}\ \mathrm{pc}^{-3}/\mathrm{yr}$ (Pottasch, 1984; see also Daub, 1982; Mallik, 1983), the average lifetime of PPNe must be $t_t \gtrsim 1000$ yr.

Table 5. Measured and expected number of PPNe

Dist. (kpc) →	1.0	1.5	2.0
Probable	3	5	8
Possible	4	9	15
For $dl = 2$	3	7	13

dl: local spatial density of PPNe, in units $10\,(-9)\ \mathrm{pc}^{-3}$

A1.3. Envelope dilution time

As discussed above, the opacity of the circumstellar dust is maximal when the star leaves the red giant branch. One expects $A \sim 50$–100 mag, A being the extinction for the star emission in the visible and UV in that moment (such values have been observed in very evolved AGB stars or young PPNe; e.g. Jura and Morris, 1985; Bedijn, 1987). When the dust envelope dilution starts, A follows the law

$$A(t) \propto 1/R_i(t) = 1/(R_0 + Vt) \sim 1/Vt.$$

R_i being the envelope inner radius, $R_0 = R_i(t=0)$, V, the (constant) expansion velocity, and t, the time elapsed from the superwind quenching. Then,

$$A(t)/A(0) \sim R_0/Vt.$$

We shall adopt for the above parameters the following canonical values: $A(0) \sim 50$–100 mag; $R_0 \sim 5$–$10\ 10^{14}$ cm, since it is known that the circumstellar grains form only at a distance of some stellar radii (e.g. Papoular and Pégourié, 1986; see also discussion in Bujarrabal et al., 1986); $V \sim 15\ \mathrm{km\,s}^{-1}$ (e.g. Knapp and Morris, 1985, this paper). We get $A(t_d) \sim 1$ mag, for $t_d \sim 1000$ yr (with a factor two of uncertainty). This magnitude, t_d, then measures the time necessary for an envelope similar to those observed in very evolved red stars to become, just by dilution, an envelope similar to those observed in PNe. Accordingly, t_d can be considered as an approximation to the transit time. We also obtain $t_t \sim 1000$ yr following this method.

A2. Conclusion

Our three methods have yielded compatible values for the transit time, in spite of the large uncertainties present, which must be considered as a consistency proof. (It is in particular remarkable that the number of known PPNe at small distances is only somewhat smaller than the spatial density necessary to explain the assumed birthrate of PNe.) We conclude that the value $t_t \sim 1000$ yr can be considered as a good measure of the transit time from AGB stars to planetary nebulae, with an estimated uncertainty of a factor of two.

In any case, this value is an average, and we stress that it may differ for stars of different masses, the transit time being probably smaller than the average for the heavy objects. However, we think

that the above mentioned factor of two includes the dispersion for the bulk of the PPNe. Transit times smaller than 500 yr (unless if they hold just for a small group of objects) could not explain the relatively large number of PPNe already detected, and even seem small when compared with the analysis of ages of well studied PPNe in Sect 3. Transit times larger than 2000 years would be in contradiction with the measured kinematical times for a wide range of PNe (or with the current ideas on late stages of stellar evolution). Nevertheless, we note that large uncertainties are present in the PNe birthrate: the PN local abundance seems well known, but the PN lifetime is a delicate parameter, whose determination may be biased towards high-mass strong emitters (as so often happens in astronomy), which probably need more time to dissipate their nebulae. If the PN birthrate is larger than the adopted value by a significant factor, we would have to admit that other low-mass objects, besides "usual" PPNe, also evolve to PNe, and that something is wrong in the interpretation of the PN kinematic times.

On the other hand, we cannot exclude other possible evolutionary paths for evolved red stars, which may not always lead to PNe. Jura (1986) has proposed that RV Tau stars represent a possible evolutionary path through the main sequence coexistant with the "usual" PPNe. Following Jura, RV Tau objects may constitute the evolution of low mass AGB stars that do not enter the superwind regime, presenting maximal mass loss rates of about $10^{-5} M_{\odot}$/yr. The evolution of the central star seems quite slow in RV Tau objects, since 500 yr after the end of the mass loss phase they still remain as late type (F, G, K) stars, see also Schönberner (1986). It is probable that the evolution of a good fraction of these objects will never produce a PN, their relatively diffuse envelopes being practically dissipated before the stars become hot enough to ionize them. (We note that it is unlikely for the PPNe we are dealing with to follow a similar evolution: most of the PPNe listed in Table 4 already present characteristics of PNe, particularly traces of an increasing ionization in a thick envelope, and seem certainly close to arriving at the PN stage.)

Acknowledgements. We remain very grateful to the Pico de Veleta technical staff for their warm support during the observations, and to A. Barcia for critical reading of the manuscript. This work has been partially supported by CAICYT, project number 477/84.

References

Allen, D.A.: 1978, *Monthly Notices Roy. Astron. Soc.* **184**, 601

Allen, D.A., Hyland, A.R., Caswell, J.L.: 1980, *Monthly Notices Roy. Astron. Soc.* **192**, 505

Aspin, C., McLean, I.S.: 1984, *Astron. Astrophys.* **134**, 333

Bachiller, R., Gómez-González, J., Bujarrabal, V., Martín-Pintado, J.: 1988, *Astron. Astrophys.* **196**, L5 (Paper I)

Baud, B.: 1981, *Astrophys. J.* **250**, L79

Beckwith, S., Beck, S.C., Gatley, I.: 1984, *Astrophys. J.* **280**, 648

Bedijn, P.J.: 1987, *Astron. Astrophys.* **186**, 136

Bujarrabal, V., Guélin, M., Morris, M., Thaddeus, P.: 1981, *Astron. Astrophys.* **99**, 239

Bujarrabal, V., Planesas, P., Gómez-González, J., Martín-Pintado, J., del Romero, A.: 1986, *Astron. Astrophys.* **162**, 157

Calvet, N., Cohen, M.: 1978, *Monthly Notices Roy. Astron. Soc.* **182**, 687

Cohen, M.: 1983, in *Planetary Nebulae*, *IAU Symp.* **103**, Reidel, Dordrecht

Cohen, M., Schmidt, G.D.: 1982, *Astrophys. J.* **259**, 693

Cohen, M., et al.: 1975, *Astrophys. J.* **196**, 179

Cohen, M., FitzGerald, M.P., Kunkel, W., Lasker, B.M., Osmer, P.S.: 1978, *Astrophys. J.* **221**, 151

Daub, C.T.: 1982, *Astrophys. J.* **260**, 612

Deguchi, S., Claussen, M.J., Goldsmith, P.F.: 1986, *Astrophys. J.* **303**, 810

Deguchi, S., Uyemura, M.: 1984, *Astrophys. J.* **285**, 153

Diamond, P.J., Norris, R.P., Booth, R.S.: 1983, *Astron. Astrophys.* **124**, L4

Diamond, P.J., Norris, R.P., Rowland, P.R., Booth, R.S., Nyman, L.-A.: 1985, *Monthly Notices Roy. Astron. Soc.* **212**, 1

Goldsmith, P.F., Krotov, R., Snell, R.L.: 1985, *Astrophys. J.* **299**, 405

Goodrich, R.W., Dahari, O.: 1985, *Astrophys. J.* **289**, 342

Gottlieb, E.W., Liller, W.: 1976, *Astrophys. J.* **207**, L135

Guélin, M.: 1987, in *Molecules in Physics, Chemistry and Biology*, Reidel, Dordrecht

Habing, H.J., van der Veen, W.: 1986, in *Late Stages of Stellar Evolution*, Proc. Workshop Held in Calgary, Reidel, Dordrecht

Heckert, P.A., Zeilik, M.: 1983, *Monthly Notices Roy. Astron. Soc.* **202**, 531

Herbig, G.H.: 1975, *Astrophys. J.* **200**, 1

Jewitt, D.C., Danielson, G.E., Kupferman, P.N.: 1986, *Astrophys. J.* **302**, 727

Jura, M., Morris, M.: 1985, *Astrophys. J.* **292**, 487

Jura, M.: 1986, *Astrophys. J.* **309**, 732

Kawabe, R., Ishiguro, M., Kasuga, T., Morita, K-I., Ukita, N., Kobayashi, H., Okomura, S., Fomalont, E.B., Kaifu, N.: 1987, *Astrophys. J.* **314**, 322

Knapp, G.R., Phillips, T.G., Leighton, R.B., Lo, K.Y., Wannier, P.G., Wootten, H.A., Huggins, P.J.: 1982, *Astrophys. J.* **252**, 616

Knapp, G.R., Chang, K.M.: 1985, *Astrophys. J.* **293**, 281

Knapp, G.R., Morris, M.: 1985, *Astrophys. J.* **292**, 640

Knapp, G.R.: 1986, *Astrophys. J.* **311**, 731

Kwok, S., Bignell, R.C.: 1984, *Astrophys. J.* **276**, 544

Kwok, S., Purton, C.R., Matthews, H.E., Spoelstra, T.A.T.: 1985, *Astron. Astrophys.* **114**, 321

Kwok, S.: 1986, in *Late Stages of Stellar Evolution*, Proc. Workshop in Calgary, Reidel, Dordrecht

Kwok, S., Hrivnak, B.J., Milone, E.F.: 1986, *Astrophys. J.* **303**, 451

Lafont, S., Lucas, R., Omont, A.: 1981, *Astron. Astrophys.* **106**, 201

Likkel, L., Omont, A., Morris, M., Forveille, T.: 1987, *Astron. Astrophys.* **173**, L11

Lo, K.Y., Bechis, K.P.: 1976, *Astrophys. J.* **205**, L25

Lucas, R., Omont, A., Guilloteau, S., Nguyen-Q-Rieu: 1986, *Astron. Astrophys.* **154**, L12

Malik, D.C.V.: 1983, in *Planetary Nebulae*, *IAU Symp.* **103**, Reidel, Dordrecht

Martín-Pintado, J., Bujarrabal, V., Planesas, P., Gómez-González, J., Bachiller, R.: 1988, *Astron. Astrophys.* **197**, L15 (Paper II)

Morris, M.: 1975, *Astrophys. J.* **197**, 603

Morris, M., Guilloteau, S., Lucas, R., Omont, A.: 1987, *Astrophys. J.* **321**, 888

Ney, E.P., Merrill, K.M., Becklin, B.E., Neugebauer, G., Wynn-Wylliams, C.G.: 1975, *Astrophys. J.* **198**, L129

Nguyen-Q-Rieu, Bujarrabal, V., Olofsson, H., Johansson, L.E.B., Turner, B.E.: 1984a, *Astrophys. J.* **286**, 276

Nguyen-Q-Rieu, Graham, D., Bujarrabal, V.: 1984b, *Astron. Astrophys.* **138**, L 5
Papoular, R., Pégourié, B.: 1986, *Astron. Astrophys.* **156**, 199
Pottasch, S.R.: 1984, in *Planetary Nebulae*, Reidel, Dordrecht
Renzini, A.: 1983, in *Planetary Nebulae*, *IAU Symp.* **103**, Reidel, Dordrecht
Rouan, D., Omont, A., Lacombe, F., Forveille, T.: 1988, *Astron. Astrophys.* **189**, L 3
Schmidt, G.D., Cohen, M.: 1981, *Astrophys. J.* **246**, 444
Schönberner, D.: 1986, in *Late Stages of Stellar Evolution*, Proc. Workshop in Calgary, Reidel, Dordrecht
Scoville, N.Z., Kwan, J.: 1976, *Astrophys. J.* **206**, 718
Silvestro, G., Robberto, M.: 1986, in *Planetary and Protoplanetary Nebulae: from IRAS to ISO*, Proc. of the Frascati Workshop, Reidel, Dordrecht
Soptka, R.J., Hildebrand, R., Jaffe, D.T., Gatley, I., Roellig, T., Werner, M., Jura, M., Zuckerman, B.: 1985, *Astrophys. J.* **294**, 242
Taylor, K.N.R., Scarrot, S.M.: 1980, *Monthly Notices Roy. Astron. Soc.* **193**, 321
Toombs, R.I., Becklin, E.E., Progel, J.A., Law, S.K., Porter, E.C., Westphal, J.A.: 1972, *Astrophys. J.* **173**, L 71
Wannier, P.G., Sahai, R.: 1987, *Astrophys. J.* **319**, 367
Wannier, P.G., Leighton, R.B., Knapp, G.R., Redman, R.O.: 1979, *Astrophys. J.* **230**, 149
Westbrook, W.E., Becklin, E.E., Merrill, K.M., Neugebauer, G., Schmidt, M., Willner, S.P., Wynn-Williams, C.G.: 1975, *Astrophys. J.* **202**, 407
Zuckerman, B., Dyck, H.M.: 1986, *Astrophys. J.* **311**, 345